



Eutherian morphological disparity across the end-Cretaceous mass extinction

THOMAS JOHN DIXON HALLIDAY^{1,2*} and ANJALI GOSWAMI^{1,2}

¹Department of Earth Sciences, University College London, Gower Street, London, WC1E 6BT, UK

²Department of Genetics, Evolution, and Environment, University College London, Gower Street, London, WC1E 6BT, UK

Received 17 June 2015; revised 12 October 2015; accepted for publication 13 October 2015

In the aftermaths of mass extinction events, during radiations of clades, and in several other evolutionary scenarios, there is often a decoupling of taxonomic diversity and morphological disparity. The placental mammal radiation after the end-Cretaceous mass extinction is one of the archetypal adaptive radiations, but the change in morphological disparity of the entire skeleton has never been quantified across this important boundary. We reconstruct ancestral morphologies of 680 discrete morphological characters onto dated phylogenies of 177 mostly Cretaceous and Palaeogene eutherians (placental mammals and their stem relatives). Using a new approach to incorporate morphologies representing ghost lineages, we assess three measures of morphological disparity (sum of ranges, sum of variances and mean pairwise dissimilarity) across stage-level time bins within the Cretaceous and Palaeogene. We find that the range-based metric suggests that eutherian disparity increased immediately after the end-Cretaceous mass extinction, while both variance-based metrics declined from the Campanian to the Maastrichtian, but showed no change in disparity from the Maastrichtian to the Puercan – the first North American Land Mammal Age of the Paleocene. Increases in variance-based metrics lag behind the range-based metric and per-lineage accumulation rate, suggesting that the response of mammals to the Cretaceous–Palaeogene event was characterized by an early radiation that increased overall morphospace occupation, followed later by specialization that resulted in increased dissimilarity. © 2015 The Authors. Biological Journal of the Linnean Society published by John Wiley & Sons Ltd on behalf of Linnean Society of London, *Biological Journal of the Linnean Society*, 2016, 118, 152–168.

KEYWORDS: evolution – Mammalia – palaeontology – Placentalia – radiation.

INTRODUCTION

Mass extinction events have long been suggested to be important drivers of evolutionary novelty. The term ‘adaptive radiation’ was coined by Osborn (1902) in specific reference to the sudden appearance in the fossil record of a whole suite of new species, and new morphologies, of placental mammals in the earliest Cenozoic, in the wake of the end-Cretaceous mass extinction. In several North American localities, the make-up of the mammalian fauna changed dramatically (Lillegraven & Eberle, 1999; Wilson, 2005), and there has long been speculation on the origin of new dietary guilds in the earliest Cenozoic (Archibald, 1983; Gunnell *et al.*, 1995; Clemens, 2002). Adaptive radiation is an evolutionary process

in which a clade undergoes an increase in lineage diversification as a result of adapting to a number of new niches (Schluter, 2000), with divergent selection for specialization to those niches promoting reproductive isolation (Rice, 1987; Barton, 2010), and hence speciation. The rate of origination of placental mammal lineages in the earliest Cenozoic has been shown to be considerably higher than later periods of the Cenozoic (Alroy, 2009). During the course of an adaptive radiation, as a result of the combined effects of speciation and specialization, it should be expected that the disparity of a clade – a measure of morphological variation (Wills, Briggs & Fortey, 1994) – should increase as the clade fills new regions of morphospace (Foote, 1994). However, it has also been suggested that a general feature of radiations is an initial decoupling between disparity and taxic diversity (Foote, 1997b; Ruta *et al.*, 2013), a pattern

*Corresponding author. E-mail: thomas.halliday.11@ucl.ac.uk

that has been observed in several invertebrate groups (Bapst *et al.*, 2012; Hopkins, 2013), where speciation increases taxic richness early on, while changes in morphological disparity react more slowly.

Taxonomic radiations can be driven by several factors. For example, a ‘key innovation’ might allow for the exploration of a novel ecosystem or niche, resulting in increased levels of taxonomic diversity as well as morphological disparity. Alternatively, a model of ecological release suggests that some extinction event in one part of the ecospace has removed the incumbent taxon, allowing a new clade to radiate and replace it (Slater, 2013). Under this model, limited initial competition within a novel environment or niche allows ‘experimentation’ of diverse morphologies, until the available ecospace is filled, and the amount of disparity levels off or decreases as ecological and/or developmental constraints limit later variation (Simpson, 1944; Schluter, 2000; Freckleton & Harvey, 2006). A different result would be expected where occupation of a new niche occurs as a taxon merely extends a geographical range – for example, in the colonization of a new island, allopatric speciation would result in an increase in diversity, but if each island is environmentally similar, a dramatic increase in disparity is unlikely. There are many other possible causes for concordant or discordant patterns of taxonomic diversity and morphological disparity (Foote, 1997b), but here we focus specifically on the case of the apparent adaptive radiation of eutherian mammals after the end-Cretaceous mass extinction and assess morphological disparity through this event.

Disparity can be measured in a number of ways. Morphometric disparity measures the variation in the shape of a feature, whether that feature is an individual element or an entire organism (Foote, 1989, 1990). The relationship between form and function is, however, complex, and many forms may result in the same function. Biomechanical disparity therefore describes the variance in the function of the feature in question, to address differences in ecology (Wainwright, 2007; Anderson, 2009). Finally, the disparity in the combinations of discrete morphological traits may be measured, which gives a metric of overall morphological similarity of a whole organism (Wills *et al.*, 1994). For any of these metrics, the superimposition of a tree allows the measurement of disparity across the topology, placing the results in a cladistic context, and allowing interpretation of how disparity changes through a clade’s evolution. An increase in disparity over the course of the lifetime of a clade has been observed in several groups, using a phylogenetic framework with each of these different metrics of disparity – discrete (Thorne, Ruta &

Benton, 2011; Hughes, Gerber & Wills, 2013), morphometric (Friedman, 2010; Young *et al.*, 2010; Prentice, Ruta & Benton, 2011; Sallan & Friedman, 2012) and biomechanical (Anderson *et al.*, 2011; Stubbs *et al.*, 2013), where some form of evolutionary radiation has been identified. Metrics of disparity may not be independent, with an association between discrete and functional (Anderson & Friedman, 2012), and between discrete and morphometric measures of disparity (Hetherington *et al.*, 2015), although morphological and biomechanical disparity measures are often different (Anderson, 2009).

It might seem obvious that an increase in disparity occurred during the original adaptive radiation – the Paleocene diversification of placental mammals. The first specialized carnivorous eutherians, as well as the first large-bodied herbivores, arose in the early Paleocene (Von Koenigswald, Rensberger & Pretzschner, 1987; Alroy, 1998; Smith *et al.*, 2010; Archibald, 2011). Variation in body size increased substantially across the Cretaceous–Palaeogene (K–Pg) boundary, as did mean body size (Alroy, 1998, 1999). Ecological release in terms of body size evolution of eutherians has also been identified (Slater, 2013), concluding that the end-Cretaceous mass extinction allowed mammals to radiate into a greater range of body sizes than had previously been available due to reduced competition (mainly from generally larger dinosaurs). This line of evidence, too, would imply that the end-Cretaceous mass extinction resulted in an overall increase in eutherian disparity. Moreover, an increase in dental disparity has been shown to have occurred in multituberculates, another major group of mammals that survived the end-Cretaceous mass extinction (Wilson *et al.*, 2012). One might therefore have expected molar shape disparity to follow a similar pattern, with the origin of many new dietary niches. Wilson (2013) demonstrated a moderate decline in both dental shape and body size disparity for mammals from the Cretaceous to the Palaeogene, but Grossnickle & Luo (2014) concluded that there was no statistical change in lower molar shape disparity in eutherians (placentals and their stem relatives).

Here, we conduct an analysis of discrete character disparity (Foote, 1992; Wills *et al.*, 1994) for a large sample of Cretaceous and Palaeogene eutherians to reconstruct disparity in a phylogenetic framework across the K–Pg boundary. Discrete characters have been used to measure disparity in diverse clades, including radiations of echinoderms (Foote, 1992), dinosaurs (Brusatte *et al.*, 2008), gnathostomes (Anderson & Friedman, 2012) and crocodylomorphs (Toljagic & Butler, 2013) and allow quantification of disparity across a broad range of morphological features and elements, as well as allowing for missing

data. We use a phylogenetic framework to assess morphological disparity of both sampled fossil and reconstructed ancestral morphologies, termed ‘cladistic disparity’ by Lloyd (2014, 2015). This method of using characters originally intended for phylogenetic analysis to calculate disparity metrics is robust to differences in coding strategy and definitions of homology, and are as appropriate for assessing disparity as traditional geometric methods (Hetherington *et al.*, 2015). Although it has been suggested that cladistic characters are only weakly associated with functional morphology (Anderson & Friedman, 2012), the convergent evolution of several morphological solutions with the same functional outcome nonetheless represents a great deal of morphological variation, and hence a change in disparity.

By quantifying three metrics of disparity across a phylogeny of Cretaceous and Paleocene mammals, we aim to determine whether the end-Cretaceous mass extinction effected a change in total cladistic disparity in eutherian mammals.

MATERIAL AND METHODS

SAMPLING

Taxa and characters were drawn from a cladistic data matrix comprising 680 morphological characters and 177 genera. Of these characters, 235 were dental, 264 cranial, and 181 postcranial, representing morphological variation across the entire skeleton and dentition. Continuous characters were treated in two ways, left as continuous or discretized. For the quantification of disparity conducted in this analysis, all 48 continuous traits were discretized such that the data matrix is exclusively discrete. Of the taxa that were included, 135 were Palaeogene and 28 Cretaceous. Taxa were drawn from across the eutherian tree, with representatives of the majority of extant placental orders, as well as most extinct Mesozoic and Cenozoic eutherian clades. In addition to the crown placental orders, Paleocene stem members of these orders and Cretaceous eutherians, two outgroup taxa were included for generation of the phylogenetic trees and optimization of ancestral character states: the stem therian *Peramus* and the metatherian *Deltatheridium*, although neither was included in calculation of the disparity metrics.

PHYLOGENETIC TREE

The dataset described above has recently been constructed and analysed to establish the phylogenetic relationships of early crown placental mammals under various levels of constraint to account for topologies supported primarily by molecular data

(Halliday *et al.*, in press). The constraints applied to the analyses ensured the monophyly of the four superordinal clades of placental mammals that are well supported by molecular data – Afrotheria (elephants, hyraxes, manatees, tenrecs), Xenarthra (sloths, armadillos, anteaters), Laurasiatheria (cats, horses, moles, bats, pangolins, whales) and Euarctoglires (primates, rodents, rabbits, colugos) – as well as the monophyly of the majority of extant placental orders. Three levels of constraint were used – a ‘full’ constraint incorporating all unambiguous members of extant placental orders, a ‘minimum’ constraint incorporating a reduced subset of these unambiguous members and a third constraint designed to test the possibility that the enigmatic Paleocene genus *Purgatorius* was a stem primate. Each constraint was applied to both entirely discrete and combined discrete–continuous datasets; the six analyses produced a total of 564 most parsimonious trees (MPTs). The differing levels of constraint and variations in the resultant MPTs used in the following analyses thus provide a robust estimate of the sensitivity of results to tree topology. These trees were subsequently dated using cal3 (Bapst, 2013) – a recently described stochastic method – incorporating occurrence data from the Palaeobiology Database (www.paleobiodb.org); these dated topologies are available in Supporting Information (Data 1–6). The stochastic method used to date the internal nodes of the trees required randomization of taxon first appearance dates within known ranges. For each of the six constraints, 50 dated trees were randomly selected for ancestral reconstruction, totalling 300 trees from which metrics of disparity could be quantified.

ANCESTRAL STATE RECONSTRUCTION

Ancestral states were reconstructed for every state and for every node using maximum-likelihood methods as implemented in the R packages *ape* (Paradis, Claude & Strimmer, 2004) and the re-rooting method of Yang, Kumar & Nei (1995) as implemented in *Claddis* (Lloyd, 2014), using the discrete character matrix described above (Supporting Information, Data 7). Ordered multistate characters were treated as such for all character reconstructions and for calculation of disparity metrics, and, to ensure internal consistency, character weightings were identical to those which generated the phylogenetic trees used in these analyses. Although the morphological characters associated with ancestral nodes are reconstructions, they ultimately represent approximations to hypothesized organisms, assuming that the phylogeny is accurate, and that a bifurcating tree is an accurate representation of the clade’s evolutionary

history. Given that ancestors necessarily existed as living species, those species would be expected to have some autapomorphic traits, subsequently lost in both descendant lineages, but these cannot be coded as the taxa have not been sampled (Brusatte *et al.*, 2011). If autapomorphies were to be coded for terminal taxa, metrics would not be comparable between nodes and tips, and bins with a higher proportion of internal nodes would tend to have artificially reduced morphological disparity relative to bins with fewer internal and more terminal nodes. Regardless of whether autapomorphies were present in any given unsampled ancestor, it has been shown that principal coordinates analysis (PCO) matrices including and excluding autapomorphies are not significantly different (Cisneros & Ruta, 2010; Close *et al.*, 2015). Therefore, for consistency between tip and node morphologies, no autapomorphic characters for any terminal taxon were included in these analyses.

GHOST LINEAGES

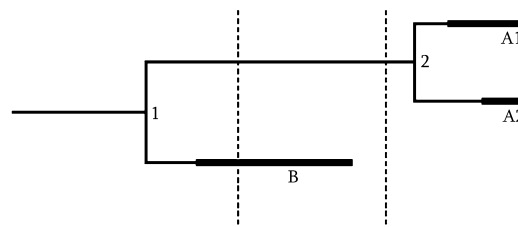
Many methods that have attempted to reconstruct changes in disparity have used only those taxa which are present in the fossil record. However, this is problematic, because, even where taxa are unknown from the fossil record, they may often be expected to be present, given a phylogenetic hypothesis, due to reconstructed ghost lineages. Several authors (Wills, 1998; Brusatte *et al.*, 2011) have identified this problem and corrected for it by reconstructing ancestral states for ancestral nodes, and including each hypothetical morphology in the single time bin in which it was reconstructed as occurring.

While an improvement on most previous methods, this is not necessarily ideal, however, as a reconstructed ancestral node will only be sampled in a single bin. It is a hypothetical combination of character states which, by definition, has no fossil record, and is therefore typically represented as solely a point in time. Tip taxa will usually range from their first to last appearance, and, depending on the method used to reconstruct extinction time (if any), even beyond these boundaries. However, occurrence ranges have not usually been implemented for reconstructions of internal ancestral nodes. A related problem is that this approach reconstructs inferred ranges for tip taxa and point occurrences for ancestral nodes, but does not fully account for ghost lineages.

Where ghost lineages are small, and the fossil record relatively complete in the period of interest, excluding ghost lineages is unlikely to substantially affect results. Ancestors are binned either with their oldest descendant (the ‘conservative’ method) or with their oldest sister taxon (the ‘punctuational’ method), depending on method (Brusatte *et al.*, 2011, 2012).

Theoretically, however, it is possible to imagine a situation (Fig. 1) where a tree spans three time bins. In the first is Node 1, an ancestor of Clade A and Clade B. Clade B is known from the first and second time bins. Clade A has two members, which diverge at Node 2 in the third time bin. These two members are known only from the third time bin. This situation is perfectly consistent with the application of the method of Brusatte *et al.* (2012), but potentially creates some undesirable circumstances. In the first time bin, we measure Node 1 and Clade B. In the second we measure Clade B. In the third, we measure Node 2, and both members of Clade A. Despite the fact that the morphology between Nodes 1 and 2 must have existed in the second time bin – assuming that the cladogram is correct – it is still not sampled by these methods, and as such will tend to underestimate disparity in such bins.

When phylogenies are dated using methods other than simply reconstructing the bins in which they appear on the basis of the raw fossil record (i.e. without applying suitable statistical corrections based on sampling), the incidence of ghost lineages passing through time bins without speciation is much higher. Any method which does not allow zero-length branches (whether from an arbitrary addition of minimum branch lengths, branch-splitting methods or



Model	Bin 1	Bin 2	Bin 3
Richness	1	1	2
“Conservative”	1	1	3
“Punctuational”	2	1	2
“Extended punctuational”	2	2	3

Figure 1. A comparison of different measures of disparity on a hypothetical, previously dated phylogeny. In this three-time-bin example, traditional richness methods as well as those corrections applied by Brusatte *et al.* (2011) will fail to recognize the morphology of the branch leading from Node 1 to Node 2 when assessing disparity. Only by treating the ancestral morphology as occurring along the entire branch can the total morphological disparity of the time bin be assessed, including all the data. Thick lines represent species occurrences; thin lines represent ghost lineages. The root itself is not counted, as the reconstruction of characters at the root node is dependent on the next outgroup, which is not sampled.

stochastic estimation) necessarily increases the proportion of ghost lineages within the phylogeny. This effect is especially prevalent for trees which possess a combination of extinct and extant taxa, with some large time difference between the majority of the extinct clades and the present.

To address this issue, we modified the approach described above to also include ghost lineages in the calculations of disparity for the time bins through which they pass. For mathematical simplicity, we assumed that the particular combination of character states along the ghost lineage is that of the daughter node or taxon. In comparison with the ‘conservative’ and ‘punctuational’ methods of Brusatte *et al.* (2011), this is perhaps best described as an ‘extended punctuational’ approach. This approach assumes that all morphological change occurs at speciation, and while this is unlikely to be strictly true in all cases, it is certainly true that speciation by necessity involves some degree of change. By assuming that all character state transitions occur at the beginning of a branch which crosses a time-bin boundary, character transitions that might have actually occurred on the portion of a branch after that boundary are reconstructed as occurring prior to that event. This approach will, as a result, push morphologies backwards in time, and tend to bias analyses by reconstructing changes as occurring earlier than they otherwise might. However, failure to apply this correction will falsely reduce disparity in intermediate time bins. In the absence of evidence as to when character changes occur along an anagenetic lineage, this approach is an improvement over existing methods because it explicitly acknowledges the presence of a ghost lineage which almost certainly had accumulated some, although probably not all, of the morphological shifts associated with its terminal state. Alternative models of discrete character evolution where characters are acquired independently along a branch may be instructive, but require the reconstruction of a new ancestral morphology at every reconstructed character change, which poses problems both theoretically and computationally for determining how the large number of intermediate morphologies ought to be binned, and whether two subsequent morphologies on a single branch ought to contribute separately to a bin’s disparity. As such, a more punctuational model of character evolution is here preferred. For comparison, all calculations were also carried out excluding reconstructed ancestral morphologies.

TIME-BINNING DATA

Ancestral character distributions were assigned to the branches leading to each node, and branches

were treated as occurring in every time bin through which they pass, including those in which they originate and end. Time bins used were geological stages for the Cretaceous, and North American Land Mammal Ages (NALMA) for the Cenozoic. The division of nodes into the time bins through which their ancestral branch passed was carried out using code written for R (Supporting Information, Data 8) using functions from the package *paleotree* (Bapst, 2012).

Using biostratigraphic over geochronological divisions is preferable for two reasons. Firstly, the known uncertainty in sampling the ages of taxa is, with few exceptions, within a stage- or NALMA-level interval. This means that error in the precise temporal position of a taxon is minimized by using the divisions that best reflect the known temporal distribution of the sampled taxa. As there is a sampling bias in the fossil record favouring North American taxa, especially with regards to the evolution of eutherian mammals, it is more sensible to treat these divisions as the more accurate option. Secondly, as these divisions were used to assess the dating of the phylogeny in the first place, it is more consistent to use the same time bins.

As longer time bins represent a greater amount of sampling of the fossil record, it would be expected that longer time bins might have higher levels of disparity, because there is a greater chance of finding more taxa, including morphologically extreme taxa. As a result, all analyses were also carried out on equal length time bins of 2 Myr ranging from 90 to 38 Mya (from the Coniacian stage to the Duchesnean NALMA, temporally roughly equivalent to the Bartonian stage). Division of time in this way provides a more fine-scale approach that is more robust to differences in time bin duration, but risks dividing the data up more finely than the uncertainty in the dating of the fossil taxa would permit.

MEASURING AND COMPARING CLADISTIC DISPARITY

After calculating ancestral state values for all characters and all nodes using maximum-likelihood, a distance matrix of all tips and nodes was generated. Under the methods described above, the morphologies for each tip and node were assigned to the ancestral branch leading to that tip or node. PCO was applied to this distance matrix to generate a multidimensional morphospace within which measures of disparity could be assessed. Three metrics of disparity were calculated for each time bin, and for each phylogenetic tree. The mean pairwise Gower dissimilarity (Gower, 1971) between all nodes and the sum of variances of PCO scores on all axes were used as variance-based metrics of disparity. Gower disparity accounts well for heterogeneous data, such

as the combination of continuous and discrete characters, as in this dataset, and hence it is preferred over a raw distance measure. Sums of ranges of PCO scores were also calculated to quantify overall morphospace occupation. Statistics deriving from sums of ranges and variance are preferable to product-based statistics because the latter are highly sensitive to sample size (Ciampaglio, Kemp & McShea, 2001). Although range-based metrics are also susceptible to sample size biases (Foote, 1997a; Butler *et al.*, 2012), they represent a different aspect of disparity from variance-based metrics, and so are included here.

To account for sample size biases inherent to range-based metrics of disparity, rarefaction curves were produced for each time bin. For each, the sample was rarefied 100 times at all sample sizes smaller than the number of morphologies in that bin, and the mean of those values taken.

To assess the significance of differences in disparity between adjacent time bins for all measures of disparity, confidence intervals were generated for disparity within each time bin. Time-bin-specific distance matrices involved in calculating mean pairwise distances were bootstrapped with 1000 replicates such that taxa were randomly sampled with replacement. Mean pairwise distance was calculated for each bootstrapped matrix, and 5 and 95% percentiles were ascertained. PCO matrices from which sums of ranges and variances were measured were also bootstrapped in the same manner. Adjacent time bins with non-overlapping 95% confidence intervals in any given measure were considered to represent significant increases or decreases in cladistic disparity for that measure. All disparity measures and bootstrapped matrices were generated in R using existing and newly written code (Supporting Information, Data 8).

RESULTS

Rarefied sums of ranges (SOR) showed consistently that range-based disparity of eutherian taxa remained relatively low during most of the Cretaceous, before increasing between the Maastrichtian and Puercan. Values for the sum of ranges of PCO scores increase by approximately 60% across these two time bins (Figs 2, 3) for a given level of rarefaction. Sums of ranges remained high throughout the Paleocene, before declining through the Eocene. In all cases, confidence intervals for SOR disparity in the Maastrichtian and Puercan did not overlap with one another, nor did those from the Paleocene to the Eocene. This pattern was consistent for all tree topologies, including those which reconstructed earlier diversifications of crown Placentalia.

Conversely, mean pairwise distance (MPD) and sums of variances (SOV) showed no significant change in disparity over the end-Cretaceous mass extinction, whether considering stage-level bins (Figs 4, 5) and equally sized, 2 million year bins (Fig. 6). The patterns of significant increases from bin to bin were identical in both variance-based metrics for disparity. In the Cretaceous, the Campanian represented a significant increase in MPD and SOV from prior time bins in most topologies, with disparity decreasing once more into the Maastrichtian. Despite stability in variance-based disparity through the K–Pg boundary, significant increases in MPD and SOV were found from the Puercan to the Torrejonian in all optimal topologies, and sometimes from the Torrejonian to the Tiffanian, suggesting that variance-based disparity rose throughout the Paleocene. After the beginning of the Eocene, there was no significant change in either variance- or range-based disparity across any single time bin. Although MPD and SOV continued to increase, albeit not significantly, across every bin, the rate of increase decelerated in younger time bins. Confidence intervals were wider for more recent time bins, which had lower sample sizes in this study, but even the widest confidence intervals (in the Miocene Clarendonian NALMA) do not overlap with the lower estimates of variance-based disparity in the Maastrichtian.

When reconstructed ancestral morphologies were excluded, calculating disparity without any cladistic context or correction, Paleocene time bins also had consistently higher rarefied sum of range disparity than the Cretaceous. However, variance-based disparity also shows an increase across the Cretaceous–Paleocene boundary when only considering the fossil taxa. Both range-based and variance-based metrics display a similar pattern of decline during the Eocene.

MORPHOSPACE OCCUPATION

Individually, PCO axes represented extremely low proportions of overall variation between taxa. For example, PCO1 and PCO2 together represented only 3% of the total variation, regardless of tree topology. Therefore, interpretation of the meaning of any single axis is not statistically informative, and further extrapolation of ecological correlates with each PCO axis would not be justified (Fig. 7). Nonetheless, qualitative assessment of the morphospace represented by PCO axes 1 and 2, with Campanian, Maastrichtian and Puercan morphologies shown, demonstrated a distinct shift from one region of morphospace to another (Fig. 8). Campanian taxa are divided into two nearly equal-sized groups. One is

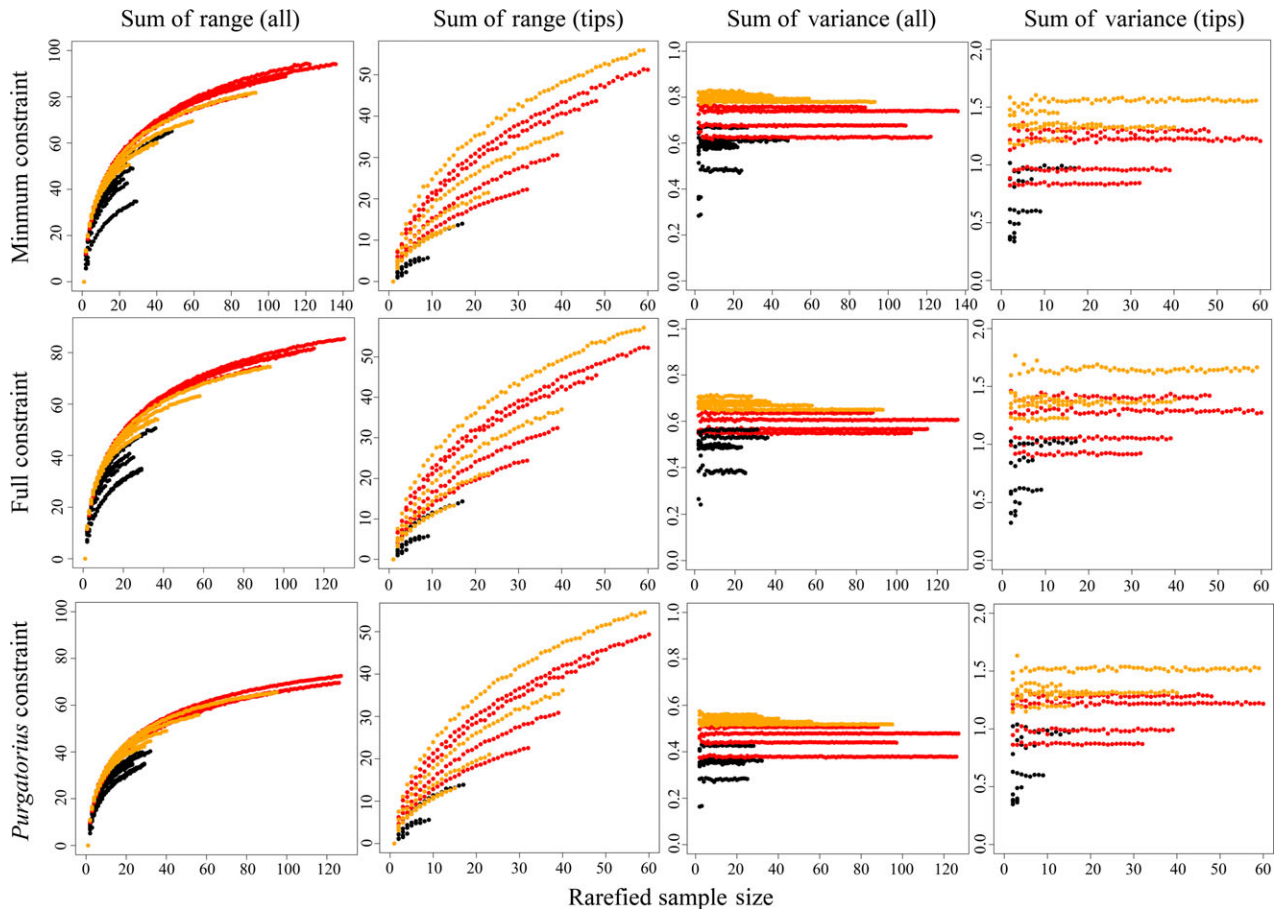


Figure 2. Rarefaction curves for sums of range and variance of PCO scores for optimal topologies under various constraints, and whether excluding ancestral morphologies or not. In each graph, the mean disparity values of 100 rarefied samples of all sizes from 1 to the full sample have been plotted for all Cretaceous (black), Paleocene (red) and Eocene (orange) bins. Cretaceous bins have typically much lower values of disparity, even when sample size is taken into account. Sums of range are highly susceptible to sample size, while sums of variance remain constant across sample sizes. In all cases, the x -axis represents sample size and the y -axis the disparity metric. Exclusion of ancestral morphologies lowers the reconstructed disparity of Paleocene and Cretaceous time bins relative to the Eocene.

clustered in the bottom left of the depicted morphospace; these are mostly zhelestids, zalambdalestids and asioryctitheres – groups of eutherians only distantly related to the crown group. In the Maastrichtian, those eutherian lineages are predominantly limited to only a single taxon or a few taxa, while other stem groups have diversified. These stem groups include Cimolestidae and Leptictida, as well as *Protungulatum*, all of which are located in a central position in the depicted morphospace. Moreover, Placentalia is reconstructed as having originated in the Maastrichtian in these topologies, meaning that a few early placental morphologies are represented in the Maastrichtian PCO plot. Placentalia and their closer relatives occupy a different part of the morphospace, in the bottom right and top left, crossing the origin. From the Campanian to the Maastrichtian, and again

from the Maastrichtian to the Puercan, the clusters of non-placental eutherians reduce in disparity or disappear entirely, while the placentals expand to occupy an increasing proportion of the eutherian morphospace.

DISCUSSION

The combination of range- and variance-based metrics of disparity described here provides a new insight into the evolutionary dynamics that characterized early placental evolution. There is a clear disjunct between patterns of range- and variance-based measures within eutherian mammals throughout the late Cretaceous and early Palaeogene. A reduction in MPD and SOV but an increase in SOR in the

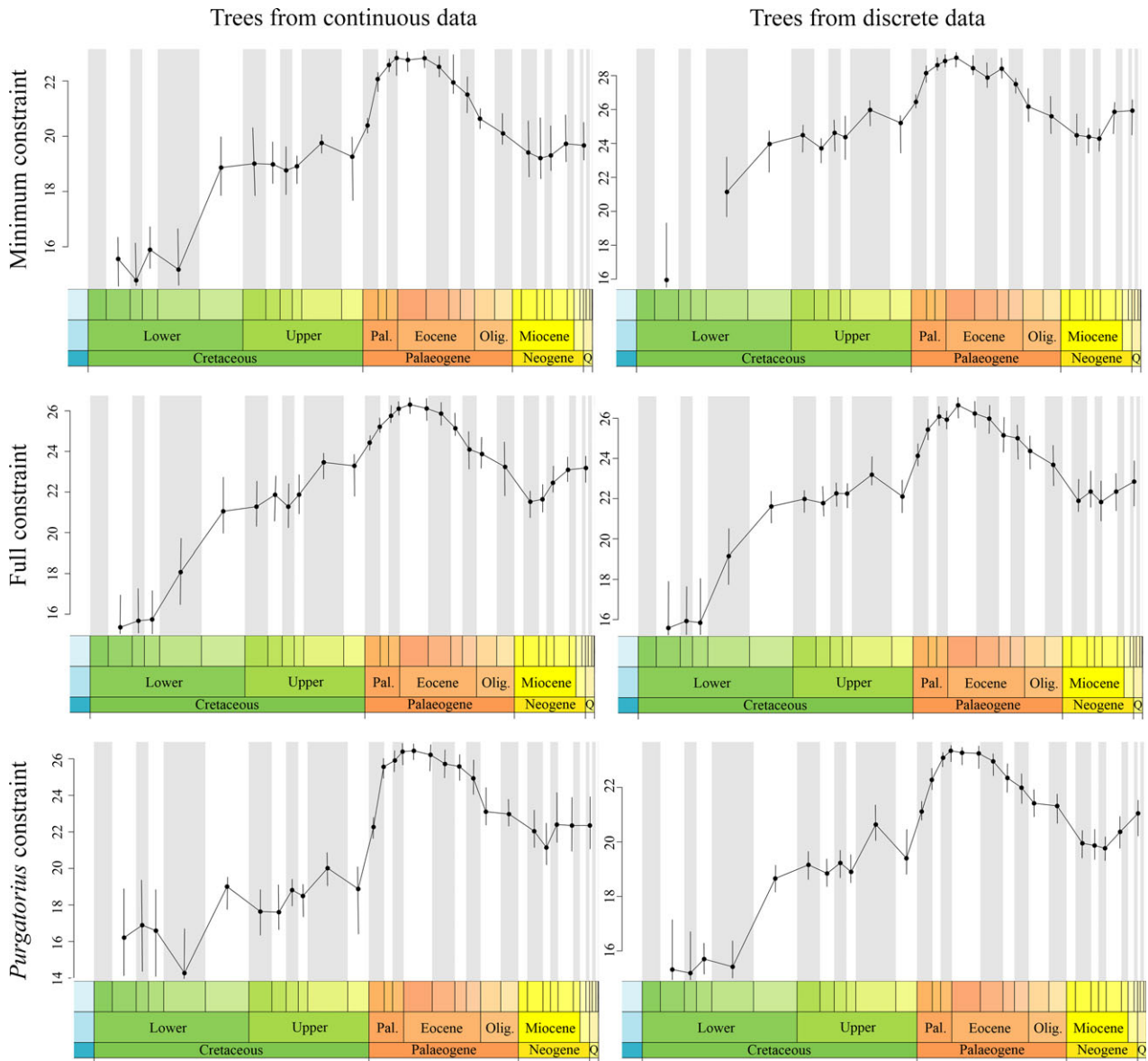


Figure 3. Time-binned measures of sum of ranges on 353 PCO axes for all sets of trees, rarefied to a standardized sample size of five bins and plotted using the R package geoscale (Bell, 2015). In all analyses the Puercan contains a larger occupied region of morphospace than the Maastrichtian, with Paleocene bins being higher in range-based disparity than later Eocene and Neogene bins. Each graph represents a tree derived from a different level of constraint.

Maastrichtian demonstrates that, while the total occupation of morphospace is increased, the majority of the variation is within a small portion of that morphospace, with higher clustering than in earlier Cretaceous stages. This pattern could arise from taxic selectivity of an extinction event, where certain portions of the morphospace are reduced (Korn, Hopkins & Walton, 2013), or from localized diversification, where several closely related, recently diverged taxa cluster morphologically. Reductions in MPD and SOV immediately following taxon-selective extinction

events are known (Bapst *et al.*, 2012), even where the surviving taxon subsequently radiates; this is indicative of a selective extinction (Foote, 1993b), which is a pattern previously noted for mammals in general at the K–Pg boundary (Wilson, 2013). However, the reduction in variance-based metrics in this analysis occurs prior to the end-Cretaceous mass extinction, requiring further consideration.

Large but peripheral subgroups contribute the greatest amount to measures of disparity (Foote, 1993a), which seems to be the case here for Placen-

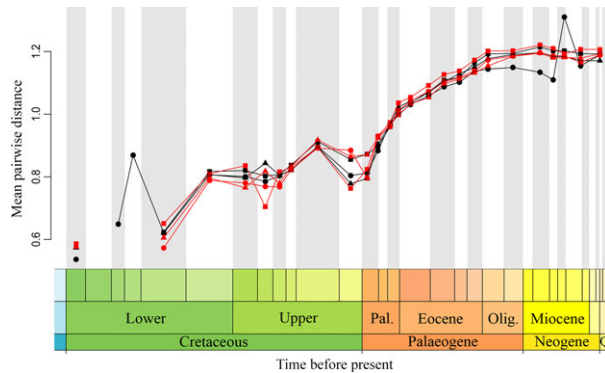


Figure 4. Time-binned measures of mean pairwise distance. Each line represents the mean pairwise distance between morphologies represented in that bin for each of the six sets of MPTs derived from continuous/discrete data, and each of three constraint topologies. Red points indicate disparity of MPTs derived from discrete-continuous datasets, and black those derived from discrete only. Circles represent those derived from a minimum constraint, triangles those from a full constraint and squares those from the *Purgatorius* constraint. There is no change between the last Cretaceous bin (Maastrichtian) and the first Paleocene bin (Puercan), but subsequent radiation in the Paleocene causes mean pairwise disparity to rise. Plotted using geoscale (Bell, 2015).

talia. Similar patterns of a reduction in variance-based metrics of disparity from the Campanian to the Maastrichtian are known for ceratopsian and hadrosaurian dinosaurs (Brusatte *et al.*, 2012). However, unlike eutherian mammals, those dinosaurs also show decreases in range-based metrics, and the pattern was spatially restricted to North America, and there is no reason to suspect that a pattern holding true for an already highly diverse, large-bodied clade such as Dinosauria would be also true of the relatively species-poor, small-bodied eutherians. Previous simulations of evolutionary radiations have suggested that low ecological diversity is to be expected at the beginning of a radiation, even where the group is relatively taxon-rich (Mitchell & Makovicky, 2014). The rise in SOR disparity in the Maastrichtian relative to the earlier Cretaceous stages therefore reflects those placental lineages which were reconstructed as diverging prior to the end-Cretaceous, leading to nodes such as the last common ancestors of Atlantogenata, Euarchontoglires, and the orders within Laurasiatheria. Mammals as a whole suffered a decline at least in dental disparity during the ‘mid’ Cretaceous (Grossnickle & Polly, 2013), which may contribute to the pattern observed here in eutherian cladistic disparity. That there is some disparification apparent in the Maastrichtian

implies that some increase in morphological diversity occurred alongside the division of Placentalia into the four superorders, before markedly increasing further with intra-superordinal diversification during the Paleocene. No fossils are known which represent stem members of any of the four superorders, but the dated phylogeny used here predicts that these hypothetical ancestors, which represent the beginnings of the morphological diversification that occurred in placental mammals, were present in the latest Cretaceous and into the very earliest Paleocene, but are unsampled. This is supported by several studies that demonstrated the mammal fauna of the earliest Paleocene of the North American Western Interior are largely composed of immigrant taxa with their Cretaceous ancestors existing elsewhere (Clemens, 2002; Wilson, 2014). This disparification of early placentals also reinvests the area of the morphospace occupied in the Campanian by close relatives of the crown group (cimolestids and leptictids), which has perhaps fuelled hypotheses that these groups are ancestral to placental orders (Kielan-Jaworowska, Cifelli & Luo, 2004; Meehan & Martin, 2010).

Other more basal eutherian taxa with respect to the crown group that are present in the Campanian are mostly lost by the Maastrichtian. The majority of the earlier Cretaceous forms are last known from the Campanian; of the taxa sampled here, only five are last known from the Maastrichtian: *Deltatheridium*, *Alostera*, *Paranyctoides*, *Batodon* and *Gypsonictops*. *Deltatheridium* is an outgroup taxon representing Metatheria (marsupials and their stem relatives), and will therefore not be considered further. *Alostera* is the latest known zhelestid [*Wania chowi*, a Paleocene form which was described as a zhelestid (Wang, 1995), was considered an anagalid by McKenna & Bell (1997)], a remnant of an earlier Cretaceous radiation. *Paranyctoides* is a morphologically plesiomorphic eutherian of unclear affinities. *Batodon* also has unknown relationships (Wood & Clemens, 2001), but has been considered a cimolestid (Kielan-Jaworowska *et al.*, 2004; Williamson, Weil & Standhardt, 2011). However, that group was not resolved as monophyletic in our recent analyses, which provided the phylogenetic trees for this study (Halliday *et al.*, in press). *Gypsonictops* is an early leptictid – a group which survived the end-Cretaceous mass extinction, eventually becoming extinct in the Neogene.

Those branches that passed through the Maastrichtian include a few disparate remnants of earlier radiations, as well as several internal branches which connect the close relatives of crown Placentalia, and the earliest divergences within the crown. The occurrence of the archaic ungulate-like eutherian *Protungulatum* in the Maastrichtian (Archibald *et al.*,

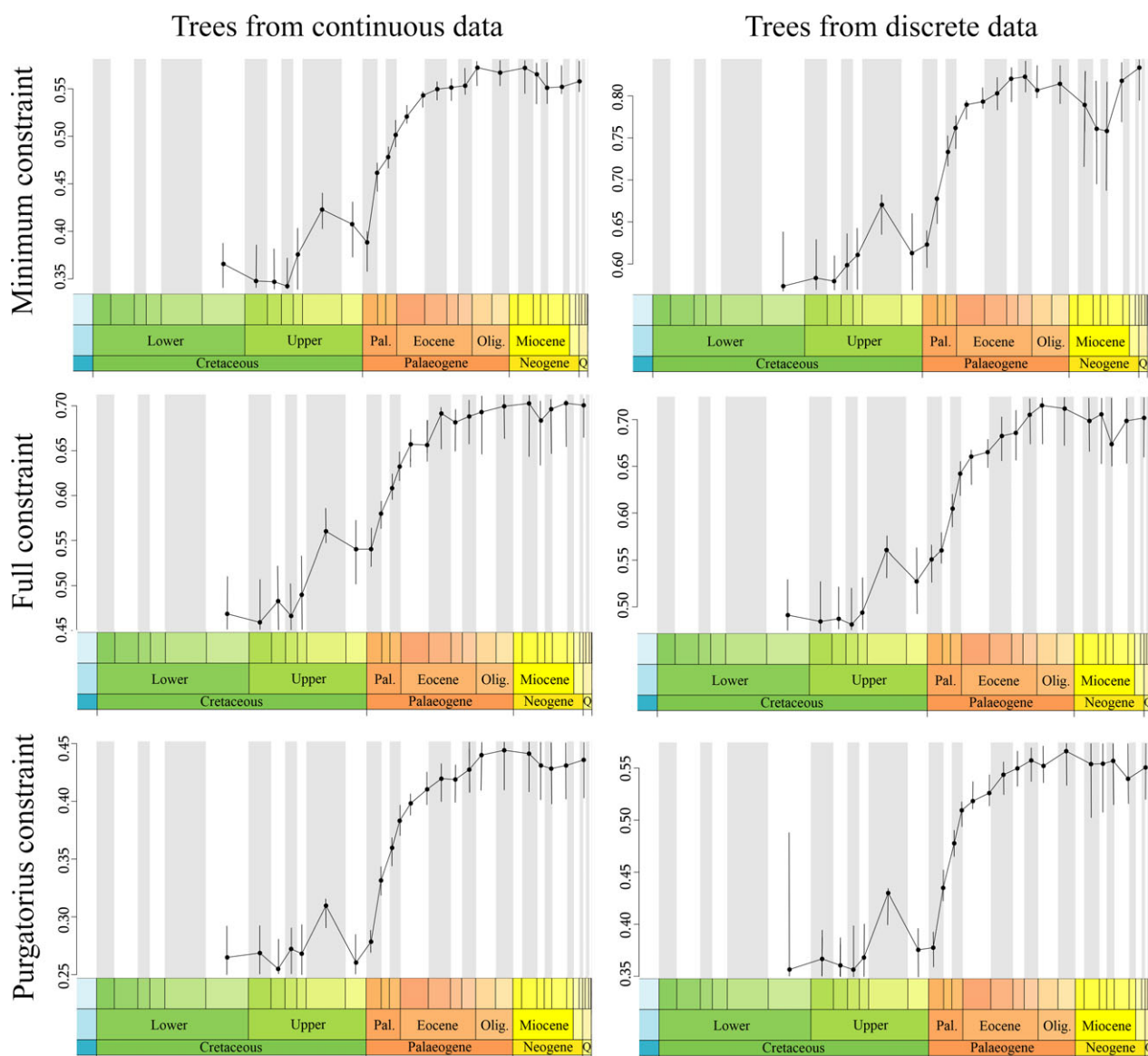


Figure 5. Sums of variances of all 353 PCO axes for each set of trees. The Campanian is a Cretaceous high, but there is no change across the end-Cretaceous mass extinction in any analysis. In the Cenozoic, variance in the PCO space increases, asymptoting approximately 40 Myr before the present. Plotted using geoscale (Bell, 2015).

2011) demonstrates that a range of placental-like morphologies already existed at this time. As a result, overall morphological space occupation increased, as some novel characters associated with the rise of placentals expanded the boundaries of the morphospace. However, as taxonomic increase was almost exclusively among close relatives and ancestors of crown Placentalia, the mean morphological distance between any pair of randomly selected taxa was smaller. Additionally, the Campanian marked the final appearance of a large number of taxa more distantly related to crown Placentalia, which results

in the region of the morphospace occupied by such taxa as *Alostera* becoming extremely depauperate. Archibald (1982, p. 259) concluded, based on the stratigraphic occurrences of Cretaceous and early Paleocene mammals, that the ‘radiation of mammals was well under way before the end of the Cretaceous’, which, when excluding those earlier groups that were in decline, has some support here in that the clade comprising Placentalia and its closest relatives began diversifying in the Maastrichtian.

Although each PCO axis explains a very low percentage of the total variation, this is typical of a

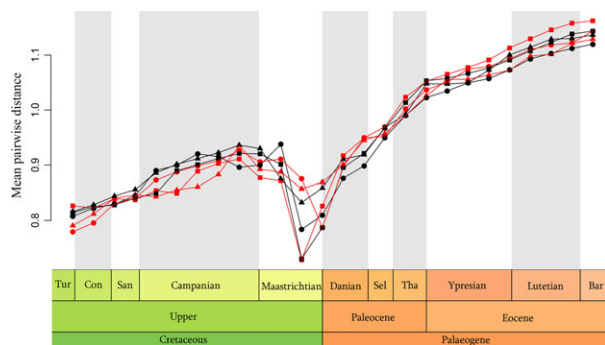


Figure 6. Mean pairwise distance across all morphologies reconstructed as being present in each 2-Myr time bin. The finer scale pattern observed here shows little change over the end-Cretaceous mass extinction, and a subsequent immediate increase. The decrease observed from the Campanian to the Maastrichtian is here found to be restricted to the period of the Maastrichtian after 70 Mya; this may be due to the uniform distribution within stages applied to first and last appearance dates when dating the tree. Colour and symbol coding as in Figure 4. Plotted using geoscale (Bell, 2015).

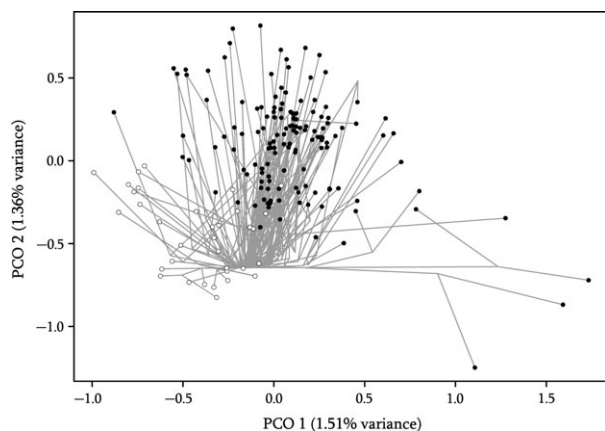


Figure 7. PCO plot of the first two coordinates axes for the cladistic distance matrix. Circles represent terminal tips – filled for crown placental mammals and open for non-placentals – and the vertices connecting the grey lines the reconstructed ancestral states from the discrete, fully constrained topology. Apart from a distinct group of edentulous mammals (the xenarthrans and pangolins), which occupy the bottom right of the plot, and a loose separation between crown and stem, no clear patterns can be drawn, and even then, the proportion of variance explained by each axis is remarkably low.

matrix composed of cladistic characters. Ideally, all morphological characters used in the generation of a cladistic data matrix are uncorrelated, meaning that each character should represent an orthogonal axis of variation in the first place. Some correlation might

be expected due to unidentified developmental association among characters and to simple biological noise, but the low percentage for the first PCO axis is expected, and is indeed reassuring, for a cladistic matrix (Goswami & Polly, 2010). Summations of ranges and variances are still meaningful, as long as they encompass most or all of the PCO axes, while keeping in mind the observation that the former is more susceptible to low sample sizes (Foote, 1997a; Butler *et al.*, 2012). While each axis explains very little of the overall variation in cladistic characters, the shifts in variance and the increase in morphospace range particularly for Placentalia and their close relatives is indicative that the Maastrichtian represents a loss of diversity in part of the eutherian tree, and the beginnings of taxonomic diversification elsewhere – a lateral extinction in the sense of Korn *et al.* (2013). The shift towards taxa more closely related to the crown group is directly supported by the fossil record, with high levels of species extinction and origination characterizing the time intervals preceding and following the end-Cretaceous mass extinction, at least at local levels (Wilson, 2014), where mammalian faunas are characterized by high levels of ‘alien’ taxa that have arrived through immigration (Archibald, 1982; Clemens, 2002), but also by speciation of new eutherian taxa in the latest Cretaceous and earliest Paleocene of North America (Archibald, 2011).

That there is neither change in mean pairwise distance nor in summed variance in morphospace across the end-Cretaceous mass extinction is perhaps surprising. However, this is simply an indication that the extinction event itself may not have been selective within Eutheria with regard to morphology. Angiosperms show a similar pattern (Lupia, 1999) of changes in taxonomic richness but not variance-based measures of disparity. However, unlike the eutherian pattern of increased range occupation but no change in variance, many vertebrate groups, such as lizards (Longrich, Bhullar & Gauthier, 2012) and multituberculates (Levering, 2013) show a dramatic decrease in range occupation – but an increase in variance-based disparity (Wilson *et al.*, 2012) – across the end-Cretaceous mass extinction, while teleost fish show a sudden increase in range occupancy and number of lineages (Friedman, 2010). While metatherian mammals were severely affected by the extinction event (Williamson, Brusatte & Wilson, 2014), the results from this study appear to suggest that eutherians went remarkably unscathed, with those groups that went extinct already in severe decline during the latest Cretaceous. This is in accord with the common observation that taxonomic richness and metrics of disparity declined substantially from the Campanian to the Maastrichtian in

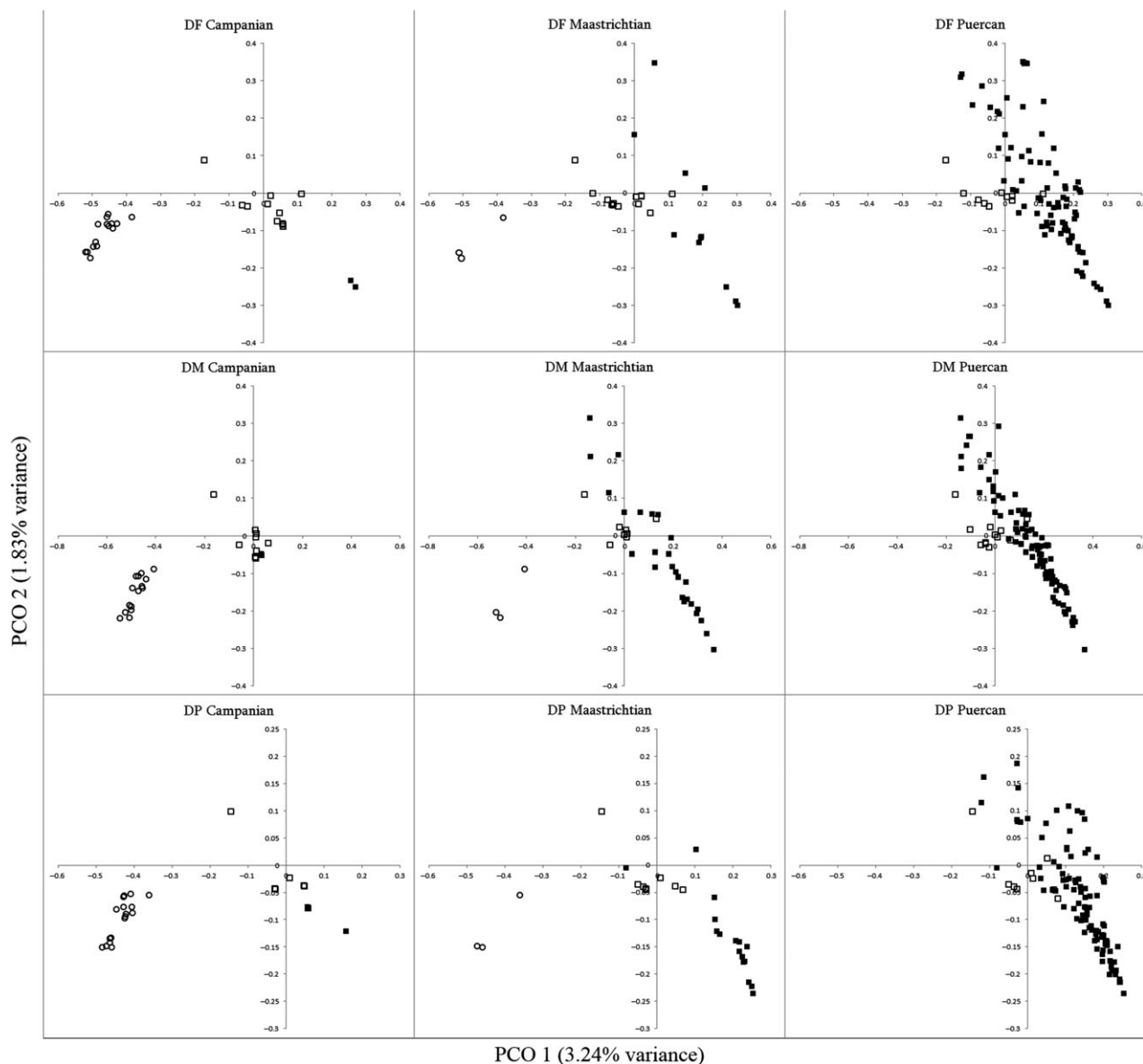


Figure 8. Morphospaces of Principal Coordinates 1 and 2, for morphologies within each time bin and for optimal topologies of discrete characters. Rows represent differing topologies, while columns represent the Campanian, Maastrichtian and Puercan, and show a pattern almost identical to Figure 8. Open circles represent basal eutherians with respect to the crown group, open squares more crownward non-placental eutherians and filled squares crown placentals. DM, discrete, minimum constraint; DF, discrete, full constraint; DP, discrete, *Purgatorius* constraint.

many mammal groups (Archibald, 1982; Kielan-Jaworowska *et al.*, 2004; Wilson *et al.*, 2012; Newham *et al.*, 2014; Williamson, Brusatte & Wilson, 2014), with the reduction in richness of Cretaceous eutherian mammals though time in the Hell Creek Formation mirroring the overall pattern in disparity observed here.

Throughout the Paleocene and Eocene, variance-based metrics of disparity increase, asymptoting to a higher level than is seen during the Cretaceous. As

this study excluded autapomorphies, increased mean pairwise distance is a result of the accumulation of synapomorphies, rendering each lineage more and more distinct. The rate at which there is an increase in MPD is therefore a measure of the rate of accumulation of synapomorphies. The characters on which this analysis was conducted were intended to differentiate between Cretaceous and Palaeogene groupings of organisms, so it may be that the slowing increase in MPD reflects the presence of fewer traits

that distinguish between intraordinal groups. Alternatively, the decelerating increase in MPD through the Cenozoic is consistent with observations from invertebrate radiations that, barring disturbances such as the immediate aftermath of extinction events, rates of evolution decline over time (Wagner, 1995; Foote, 1999). This latter observation is similar to Simpson's (1944) early burst model of adaptive radiations in rate of evolution, but contrasts in that the model predicts high morphological disparity but low taxonomic diversity early in a clade's evolution, whereas in this study morphological disparification lags behind lineage splitting and increases in taxonomic diversity. Even within the Puercan NALMA, taxonomic diversity of placental mammals in the northern Western Interior increased (Clemens, 2002), supporting the hypothesis of an extremely rapid diversification of eutherian mammals in North America.

Sustained high mean pairwise distance later in the Cenozoic may be a result of taxon sampling. As the majority of sampled taxa are from the Paleocene or Eocene, those that persist until the Recent represent relatively disparate members of the total eutherian diversity, as extinction has pruned out the intermediate taxa (Hopkins, 2013), and diversification within the crown was not thoroughly sampled. That both the end-Cretaceous and the Paleocene–Eocene boundary are turning points in mammalian disparity is consistent with previous studies. Archibald (1983) showed that rates of species turnover were highest in eutherians at these times, and both boundaries are characterized by large ecological change. Sampling also differs geographically between the Cretaceous and the Palaeogene. Approximately two-thirds of the Cretaceous taxa sampled are known from Asia, while about two-thirds of Palaeogene taxa are North American. Taxa from South America, Africa and India are only sampled in the Palaeogene, and even then only in small numbers. Although Cretaceous and Palaeogene samples are drawn from primarily different geographical regions, the spread of taxa across continents is equally broad given the known fossil record, and is unlikely to affect the estimates of morphological disparity.

Inclusion of reconstructed morphologies of ancestral nodes along hypothesized ghost lineages affects the interpretation of the results in a number of ways. When excluded, variance- and range-based patterns of disparity both show a signal of sudden increase at the end-Cretaceous mass extinction. Internal crown placental branches dated as being present in the latest Cretaceous result in little change to the reconstructed range of morphospace occupied by eutherian taxa during the Late Cretaceous and Early Palaeo-

gene time bins, but the differences in sums of variance across the K–Pg boundary are removed. Fossils are known of the taxa which represent the sequentially closest relatives of crown-group Placentalia in the Maastrichtian – for example, *Cimolestes* and *Protungulatum* – but no crown placental fossil has yet been discovered. When a taxon splits from its sister group, both lineages must be present, regardless of whether they are sampled by the fossil record. Provided that the dates reconstructed for this phylogeny are accurate, inclusion of ancestral morphologies in every bin through which they are reconstructed to have passed is both a better reflection of the known diversity in a given time bin and can produce distinct interpretations of how clades respond to evolutionary events.

The combination of changes in range- and variance-based disparity metrics and a qualitative assessment of the discrete character PCO morphospace results in a comprehensive reconstruction of late Cretaceous and early Palaeogene eutherian evolution. By the late Cretaceous, groups such as zalambdalestids, asioryctitheres and zhelestids were already in decline, perhaps as a result of ecological changes associated with the Cretaceous angiosperm radiation (Grossnickle & Polly, 2013). Most had disappeared by the end of the Campanian, while other groups, such as leptictids, cimolestids and the (currently missing) early members of Placentalia were becoming more diverse. At the end-Cretaceous mass extinction, those more basal eutherians (with respect to Placentalia) went extinct, and the surviving eutherians included Cimolestidae, Leptictidae, *Protungulatum* and Placentalia. This group taxonomically diversified rapidly, increasing the range of eutherian morphological disparity before specializing to novel ecological niches, increasing the mean pairwise distance as novel synapomorphies arose, ultimately resulting in the extraordinary ecological diversity of extant eutherians. A similar pattern is seen in multituberculates (Wilson *et al.*, 2012), where the K–Pg boundary marks a transition from less complex, more omnivorous taxa to taxa with highly complex, herbivorous dentition, alongside an increase in taxonomic richness and body size. While multituberculates had been relatively diverse and ecologically disparate prior to the end-Cretaceous mass extinction, however, the increase in diversity for eutherians shown here was unprecedented.

CONCLUSIONS

The end-Cretaceous mass extinction undoubtedly had an impact on the evolution of eutherian mam-

mals and the radiation of crown Placentalia. The earliest Paleocene is here shown to be a period in which the range of morphologies of those earliest placental taxa expanded greatly. However, taking Eutheria as a whole, the story is more complicated. Parts of the eutherian tree were already in decline prior to the end-Cretaceous mass extinction event, with the beginnings of a taxic turnover in the Maastrichtian from archaic eutherians such as zhelestids and zambdalestids to the more derived forms such as leptictids and the progenitors of Placentalia. This is manifested in the decline in mean pairwise dissimilarity from the Campanian to the Maastrichtian. The rise in SOR reflects the beginning of the diversification of Placentalia, with new synapomorphies exploring novel regions of morphospace. In the Paleocene, MPD increased as the adaptive radiation resulted in placental mammals specializing ecologically. The loss of several groups of eutherians and the subsequent radiation of others highlights the selectivity of the end-Cretaceous mass extinction. Although the extinction event caused the loss of those more basal (with respect to Placentalia) eutherians, a transition within eutherian mammals was already underway, paving the way for the subsequent radiation.

ACKNOWLEDGEMENTS

We thank Graeme Lloyd for assistance with the code, and Paul Upchurch, the ADaPTiVE discussion group and the UCL-NHM-Imperial journal club for discussion and advice. This work was funded by NERC Award NE/J/500136/1 to T.J.D.H. and Leverhulme Trust grant RPG-2014/364 to A.G. and T.J.D.H.

This paper was a contribution to a Linnean Society symposium on “Radiation and Extinction: Investigating Clade Dynamics in Deep Time” held on November 10–11, 2014 at the Linnean Society of London and Imperial College London and organised by Anjali Goswami, Philip D. Mannion, and Michael J. Benton, the proceedings of which have been collated as a Special Issue of the Journal (2016).

REFERENCES

- Alroy J. 1998.** Cope’s rule and the dynamics of body mass evolution in North American fossil mammals. *Science* **280**: 731–734.
- Alroy J. 1999.** The fossil record of North American mammals: evidence for a Paleocene evolutionary radiation. *Systematic Biology* **48**: 107–118.
- Alroy J. 2009.** Speciation and extinction in the fossil record of North American mammals. In: Butlin RK, Bridle JR, Schluter D, eds. *Speciation and patterns of diversity*. Cambridge, UK: Cambridge University Press.
- Anderson PSL. 2009.** Biomechanics, functional patterns, and disparity in Late Devonian arthropods. *Paleobiology* **35**: 321–342.
- Anderson PSL, Friedman M. 2012.** Using cladistic characters to predict functional variety: experiments using early gnathostomes. *Journal of Vertebrate Paleontology* **32**: 1254–1270.
- Anderson PSL, Friedman M, Brazeau MD, Rayfield EJ. 2011.** Initial radiation of jaws demonstrated stability despite faunal and environmental change. *Nature* **476**: 206–209.
- Archibald JD. 1982.** A study of Mammalia and geology across the Cretaceous–Tertiary boundary in Garfield County, Montana. *University of California Publications in Geological Sciences* **122**: 1–286.
- Archibald JD. 1983.** Structure of the K-T mammal radiation in North America: speculation on turnover rates and trophic structure. *Acta Palaeontologica Polonica* **28**: 7–17.
- Archibald JD. 2011.** Extinction and radiation: how the fall of dinosaurs led to the rise of mammals. Baltimore, Maryland: Johns Hopkins University Press. 108.
- Archibald JD, Zhang Y, Harper T, Cifelli RL. 2011.** *Protungulatum*, confirmed Cretaceous occurrence of an otherwise Paleocene eutherian (Placental?) mammal. *Journal of Mammalian Evolution* **18**: 153–161.
- Bapst DW. 2012.** paleotree: an R package for paleontological and phylogenetic analyses of evolution. *Methods in Ecology and Evolution* **3**: 803–807.
- Bapst DW. 2013.** A stochastic rate-calibrated method for time-scaling phylogenies of fossil taxa. *Methods in Ecology and Evolution* **4**: 724–733.
- Bapst DW, Bullock PC, Melchin MJ, Sheets HD, Mitchell CE. 2012.** Graptoloid diversity and disparity became decoupled during the Ordovician mass extinction. *Proceedings of the National Academy of Sciences of the United States of America* **109**: 3428–3433.
- Barton NH. 2010.** What role does natural selection play in speciation? *Philosophical Transactions of the Royal Society B-Biological Sciences* **365**: 1825–1840.
- Bell MA. 2015.** geoscale: Geological Time Scale Plotting. R package version 2.0. <http://CRAN.R-project.org/package=geoscale>
- Brusatte SL, Benton MJ, Ruta M, Lloyd GT. 2008.** Superiority, competition, and opportunism in the evolutionary radiation of dinosaurs. *Science* **321**: 1485–1488.
- Brusatte SL, Montanari S, H-y Yi, Norell MA. 2011.** Phylogenetic corrections for morphological disparity analysis: new methodology and case studies. *Paleobiology* **37**: 1–22.
- Brusatte SL, Butler RJ, Prieto-Marquez A, Norell MA. 2012.** Dinosaur morphological diversity and the end-Cretaceous extinction. *Nature Communications* **3**: 8.
- Butler RJ, Brusatte SL, Andres B, Benson RBJ. 2012.** How do geological sampling biases affect studies of morphological evolution in deep time? A case study of pterosaur (Reptilia: Archosauria) disparity. *Evolution* **66**: 147–162.

- Ciampaglio CN, Kemp M, McShea DW. 2001.** Detecting changes in morphospace occupation patterns in the fossil record: characterization and analysis of measures of disparity. *Paleobiology* **27**: 695–715.
- Cisneros JC, Ruta M. 2010.** Morphological diversity and biogeography of procolophonids (Amniota: Parareptilia). *Journal of Systematic Palaeontology* **8**: 607–625.
- Clemens WA. 2002.** Evolution of the mammalian fauna across the Cretaceous–Tertiary boundary in northeastern Montana and other areas of the Western Interior. In: Hartman JH, Johnson KR, Nichols DJ, eds. *Hell Creek Formation and the Cretaceous–Tertiary Boundary in the Northern Great Plains: an Integrated Continental Record of the End of the Cretaceous*. Geological Society of America Special Paper **361**: 217–245.
- Close RA, Friedman M, Lloyd GT, Benson RBJ. 2015.** Evidence for a mid-Jurassic Adaptive Radiation in Mammals. *Current Biology* **25**: 2137–2142.
- Foote M. 1989.** Perimeter-based Fourier analysis – a new morphometric method applied to the trilobite cranidium. *Journal of Paleontology* **63**: 880–885.
- Foote M. 1990.** Nearest-neighbor analysis of trilobite morphospace. *Systematic Zoology* **39**: 371–382.
- Foote M. 1992.** Paleozoic record of morphological diversity in blastozoan echinoderms. *Proceedings of the National Academy of Sciences of the United States of America* **89**: 7325–7329.
- Foote M. 1993a.** Contributions of individual taxa to overall morphological disparity. *Paleobiology* **19**: 403–419.
- Foote M. 1993b.** Discordance and concordance between morphological and taxonomic diversity. *Paleobiology* **19**: 185–204.
- Foote M. 1994.** Morphological disparity in Ordovician–Devonian crinoids and the early saturation of morphological space. *Paleobiology* **20**: 320–344.
- Foote M. 1997a.** Sampling, taxonomic description, and our evolving knowledge of morphological diversity. *Paleobiology* **23**: 181–206.
- Foote M. 1997b.** The evolution of morphological diversity. *Annual Review of Ecology and Systematics* **28**: 129–152.
- Foote M. 1999.** Morphological diversity in the evolutionary radiation of Paleozoic and post-Paleozoic crinoids. *Paleobiology* **25**: 1–115.
- Freckleton RP, Harvey PH. 2006.** Detecting non-Brownian trait evolution in adaptive radiations. *Plos Biology* **4**: 2104–2111.
- Friedman M. 2010.** Explosive morphological diversification of spiny-finned teleost fishes in the aftermath of the end-Cretaceous extinction. *Proceedings of the Royal Society B-Biological Sciences* **277**: 1675–1683.
- Goswami A, Polly PD. 2010.** The influence of character correlations on phylogenetic analyses: a case study of the carnivoran cranium. In: Goswami A, Friscia A, eds. *Carnivoran evolution: new views on phylogeny, form and function*. [Cambridge Studies in Morphology and Molecules: New Paradigms in Evolutionary Biology]. Cambridge, Cambridgeshire, UK: Cambridge University Press, 141–164.
- Gower JC. 1971.** A general coefficient of similarity and some of its properties. *Biometrics* **27**: 857–871.
- Grossnickle D, Luo ZX. 2014.** Morphological disparity patterns of Cretaceous and early Paleocene therians. *Journal of Vertebrate Paleontology*. Program and Abstracts **2014**: 141–142.
- Grossnickle DM, Polly PD. 2013.** Mammal disparity decreases during the Cretaceous angiosperm radiation. *Proceedings of the Royal Society B-Biological Sciences* **280**: 20132110.
- Gunnell GF, Morgan ME, Maas MC, Gingerich PD. 1995.** Comparative paleoecology of Paleogene and Neogene mammalian faunas – trophic structure and composition. *Palaeogeography Palaeoclimatology Palaeoecology* **115**: 265–286.
- Halliday TJD, Goswami A. 2015.** Data from: Eutherian morphological disparity across the end-Cretaceous mass extinction. Dryad Digital Repository. doi:10.5061/dryad.4d75c
- Halliday TJD, Upchurch P, Goswami A. in press.** Resolving the relationships of Paleocene placental mammals. *Biological Reviews*
- Hetherington AJ, Sherratt E, Ruta M, Wilkinson M, Deline B, Donoghue PCJ. 2015.** Do cladistic and morphometric data capture common patterns of morphological disparity? *Palaeontology* **58**: 393–399.
- Hopkins MJ. 2013.** Decoupling of taxonomic diversity and morphological disparity during decline of the Cambrian trilobite family Pterocephaliidae. *Journal of Evolutionary Biology* **26**: 1665–1676.
- Hughes M, Gerber S, Wills MA. 2013.** Clades reach highest morphological disparity early in their evolution. *Proceedings of the National Academy of Sciences of the United States of America* **110**: 13875–13879.
- Kielan-Jaworowska Z, Cifelli RL, Luo Z-X. 2004.** *Mammals from the age of dinosaurs: origin, evolutions, and structure*. New York: Columbia University Press.
- Korn D, Hopkins MJ, Walton SA. 2013.** Extinction space – a method for the quantification and classification of changes in morphospace across extinction boundaries. *Evolution* **67**: 2795–2810.
- Levering D. 2013.** *A morphological oddity: assessing morphological disparity of the Cimolodonta (Multituberculata) across the Cretaceous–Paleogene extinction boundary*. Oklahoma State University: Unpublished Master of Science.
- Lillegraven JA, Eberle JJ. 1999.** Vertebrate faunal changes through Lancian and Puercan time in southern Wyoming. *Journal of Paleontology* **73**: 691–710.
- Lloyd GT. 2015.** Estimating morphological diversity and tempo with discrete character-taxon matrices: implementation, challenges, progress, and future directions. *Biological Journal of the Linnean Society* **118**: 131–151.
- Lloyd GT. 2014.** Claddis: Cladistic disparity. R package version 0.1: Accessed 12 November 2014.
- Longrich NR, Bhullar B-AS, Gauthier JA. 2012.** Mass extinction of lizards and snakes at the Cretaceous–Paleogene

- boundary. *Proceedings of the National Academy of Sciences of the United States of America* **109**: 21396–21401.
- Lupia R. 1999.** Discordant morphological disparity and taxonomic diversity during the Cretaceous angiosperm radiation: North American pollen record. *Paleobiology* **25**: 1–28.
- McKenna MC, Bell SK. 1997.** *Classification of mammals above the species level*. New York: Columbia University Press.
- Meehan TJ, Martin LD. 2010.** New leptictids (Mammalia: Insectivora) from the Early Oligocene of Nebraska, USA. *Neues Jahrbuch Fur Geologie Und Palaontologie-Abhandlungen* **256**: 99–107.
- Mitchell JS, Makovicky PJ. 2014.** Low ecological disparity in Early Cretaceous birds. *Proceedings of the Royal Society B-Biological Sciences* **281**: 20140608.
- Newham E, Benson R, Upchurch P, Goswami A. 2014.** Mesozoic mammaliaform diversity: the effect of sampling corrections on reconstructions of evolutionary dynamics. *Palaeogeography Palaeoclimatology Palaeoecology* **412**: 32–44.
- Osborn HF. 1902.** The law of adaptive radiation. *American Naturalist* **36**: 353–363.
- Paradis E, Claude J, Strimmer K. 2004.** APE: Analyses of Phylogenetics and Evolution in R language. *Bioinformatics* **20**: 289–290.
- Prentice KC, Ruta M, Benton MJ. 2011.** Evolution of morphological disparity in pterosaurs. *Journal of Systematic Palaeontology* **9**: 337–353.
- Rice WR. 1987.** Speciation via habitat specialization: the evolution of reproductive isolation as a correlated character. *Evolutionary Ecology* **1**: 301–314.
- Ruta M, Angielczyk KD, Froebisch J, Benton MJ. 2013.** Decoupling of morphological disparity and taxic diversity during the adaptive radiation of anomodont therapsids. *Proceedings of the Royal Society B-Biological Sciences* **280**: 20131071.
- Sallan LC, Friedman M. 2012.** Heads or tails: staged diversification in vertebrate evolutionary radiations. *Proceedings of the Royal Society B-Biological Sciences* **279**: 2025–2032.
- Schluter D. 2000.** *The ecology of adaptive radiation*. Oxford: Oxford University Press.
- Simpson GG. 1944.** *Tempo and mode in evolution*. New York: Columbia University Press.
- Slater GJ. 2013.** Phylogenetic evidence for a shift in the mode of mammalian body size evolution at the Cretaceous–Palaeogene boundary. *Methods in Ecology and Evolution* **4**: 734–744.
- Smith FA, Boyer AG, Brown JH, Costa DP, Dayan T, Ernest SKM, Evans AR, Fortelius M, Gittleman JL, Hamilton MJ, Harding LE, Lintulaakso K, Lyons SK, McCain C, Okie JG, Saarinen JJ, Sibly RM, Stephens PR, Theodor J, Uhen MD. 2010.** The evolution of maximum body size of terrestrial mammals. *Science* **330**: 1216–1219.
- Stubbs TL, Pierce SE, Rayfield EJ, Anderson PSL. 2013.** Morphological and biomechanical disparity of crocodile-line archosaurs following the end-Triassic extinction. *Proceedings of the Royal Society B-Biological Sciences* **280**: 20131940.
- Thorne PM, Ruta M, Benton MJ. 2011.** Resetting the evolution of marine reptiles at the Triassic–Jurassic boundary. *Proceedings of the National Academy of Sciences of the United States of America* **108**: 8339–8344.
- Toljagic O, Butler RJ. 2013.** Triassic–Jurassic mass extinction as trigger for the Mesozoic radiation of crocodylomorphs. *Biology Letters* **9**: 1–4.
- Von Koenigswald W, Rensberger JM, Pretzschner HU. 1987.** Changes in the tooth enamel of Early Paleocene mammals allowing increased diet diversity. *Nature* **328**: 150–152.
- Wagner PJ. 1995.** Testing evolutionary constraint hypotheses with Early Paleozoic gastropods. *Paleobiology* **21**: 248–272.
- Wainwright PC. 2007.** Functional versus morphological diversity in macroevolution. *Annual Review of Ecology Evolution and Systematics* **38**: 381–401.
- Wang Y. 1995.** A new zhelestid (Mixotheridia, Mammalia) from the Paleocene of Qianshan, Anhui. *Vertebrata Palasiatica* **33**: 114–137.
- Williamson TE, Weil A, Standhardt B. 2011.** Cimolestids (Mammalia) from the Early Paleocene (Puercan) of New Mexico. *Journal of Vertebrate Paleontology* **31**: 162–180.
- Williamson TE, Brusatte SL, Wilson GE. 2014.** The origin and early evolution of metatherian mammals: the Cretaceous record. *ZooKeys* **465**: 1–76.
- Wills MA. 1998.** Crustacean disparity through the Phanerozoic: comparing morphological and stratigraphic data. *Biological Journal of the Linnean Society* **65**: 455–500.
- Wills MA, Briggs DEG, Fortey RA. 1994.** Disparity as an evolutionary index – a comparison of Cambrian and Recent arthropods. *Paleobiology* **20**: 93–130.
- Wilson GP. 2005.** Mammalian faunal dynamics during the last 1.8 million years of the Cretaceous in Garfield County, Montana. *Journal of Mammalian Evolution* **12**: 53–76.
- Wilson GP. 2013.** Mammals across the K/Pg boundary in northeastern Montana, USA: dental morphology and body-size patterns reveal extinction selectivity and immigrant-fueled ecospace filling. *Paleobiology* **39**: 429–469.
- Wilson GP. 2014.** Mammalian extinction, survival, and recovery dynamics across the Cretaceous–Palaeogene boundary in north-eastern Montana, USA. In: Wilson GP, Clemens WA, Horner JR, Hartman JH eds. *Through the End of the Cretaceous in the Type Locality of the Hell Creek Formation in Montana and Adjacent Areas, Geological Society of America Special Paper* **503**: 365–392.
- Wilson GP, Evans AR, Corfe IJ, Smits PD, Fortelius M, Jernvall J. 2012.** Adaptive radiation of multituberculate mammals before the extinction of dinosaurs. *Nature* **483**: 457–460.
- Wood CB, Clemens WA. 2001.** A new specimen and a functional reassociation of the molar dentition of *Batodon tenuis* (Placentalia, Incertae sedis), latest Cretaceous (Lancian), North America. *Bulletin of the Museum of Comparative Zoology* **156**: 99–118.
- Yang ZH, Kumar S, Nei M. 1995.** A new method of inference of ancestral nucleotide and amino acid sequences. *Genetics* **141**: 1641–1650.

Young MT, Brusatte SL, Ruta M, de Andrade MB. 2010. The evolution of Metriorhynchoidea (Mesoeucrocodylia, Thalattosuchia): an integrated approach using

geometric morphometrics, analysis of disparity, and biomechanics. *Zoological Journal of the Linnean Society* **158**: 801–859.

SUPPORTING INFORMATION

Additional Supporting Information may be found online in the supporting information tab for this article:

Data S1–6. Trees resulting from prior cladistic analysis (Halliday *et al.*, in press) and dating used in this analysis.

Data S7. Discrete character–taxon matrix used for ancestral reconstruction and generation of the tree topologies

Data S8. New R code used to run the analyses, requiring ape, geiger and Claddis packages to be installed.

Data S9. Morphospaces of Principal Coordinates 1 and 2, for morphologies within each time bin and optimal topologies derived from the combined discrete–continuous phylogenetic analyses. Open circles represent basal eutherians with respect to the crown group, open squares more crownward non-placental eutherians and filled squares crown placentals. CM, continuous, minimum constraint; CF, continuous, full constraint; CP, continuous, *Purgatorius* constraint.

SHARED DATA

Data deposited in the Dryad digital repository (Halliday *et al.*, 2015).